3D SIMULATION AND RESIDUAL STRESS ANALYSIS OF JOINING AA7075 ALLOY SHEET WITH LASER WELDING METHODS

Cenk MISIRLI[1], Isik CETINTAV[2]

[1] Trakya University

Abstract

A numerical simulation model of the laser beam welding (LBW) process has been created with the goal of estimating residual stress and distortion fields with high accuracy. Because LBW is a thermo-mechanical process, a thermal analysis is done based on a mechanical analysis to compute residual stresses and distortions. For the estimate of size and shape necessary for thermal analysis, a new and efficient model that is independent of any experimental parameter is presented. The model incorporates all of the major physical processes connected with the LBW process, such as heat radiation, thermal conduction, and convection heat losses. Due to significant temperature fluctuations and material phase shifts during welding, thermal and mechanical material characteristics are expressed as temperature-dependent functions. Within the MSC Marc Mentat finite element code, the simulation method is coded as a macro procedure.

Keywords: Laser beam welding, Keyhole modelling, Thermo-mechanical analysis, Welding simulation

INTRODUCTION

Laser beam welding (LBW) is based on high power density welding technologies that can focus beam power to a very tiny spot diameter. As a result, the LBW method is superior to traditional welding procedures such as arc welding, resulting in smaller Heat Affected Zones (HAZ), reduced distortions, residual stresses, and strains.

Most welding techniques function in conduction-limited mode, which means that the heat delivered to the surface of the irradiated material by laser light absorption is essentially transmitted to the surrounding material via conduction. When the laser power density is high a keyhole is formed, which is accompanied by phase change processes such as melting and evaporation. Because of the numerous physical processes occurring [1,] the optimization of the laser welding process often relies on welding experiments and trial and error techniques, which have many operational challenges, increasing the total cost of the process.

Simulation models of the welding process that have been validated by experimental results are critical for a variety of reasons, including a thorough understanding of the LBW physics, the reliable extension of the process applicability to modern demanding industrial applications, and the efficient definition of the LBW process parameters at a low cost.

Accurately mapping the heat input to the material is the most important issue in LBW thermal analysis. The keyhole phenomenon is mostly responsible for non-uniform localized heating of the material volume. According to experimental data, the shape of the taphole of deep penetration welding is almost conical, and the apex angle decreases as the depth of the taphole increases [12-15]. A method for mathematical modeling of keyhole formation in laser welding of steel can be found in [16,17], but no reference can be found for aluminum materials.

Many researchers have developed mathematical models of weld pool and keyhole geometries and positions in steel LBWs [18–24] by properly accounting for energy and pressure balances. However, these models are very complex and difficult to apply in practice to different geometries, materials and connection types.

In this paper, a thermo-mechanical FE model is developed to predict stress, strain and distortion fields to simulate butt joint welding of aluminum components. The main innovations of the model are an innovative keyhole prediction approach with the ability to machine any steel or aluminum alloy, as well as an advanced numerical approach that enables efficient prediction of residual stress and distortions of LBW components. Moreover, the proposed simulation methodology is particularly effective for lap- and T-joint LBW, which, although widely used in many industrial applications, is not adequately covered in the literature.

THERMO-MECHANICAL ANALYSIS

For the LBW simulation, the global coupled thermo-mechanical model assumes a three-dimensional Gaussian heat flux distribution in a conical volume that travels along the weld line. As mentioned in Section 2, this conical volume forms as an approximation of the expected keyhole. A coupled thermo-mechanical analysis may be performed using the thermal and mechanical boundary conditions, and temperature distributions, residual stresses, and distortions can be determined.

The model is illustrated below, with 580 components and 1322 nodes at first. The element type 7 with assumed strain formulation is employed in this simulation. This element captures bending better than the traditional brick element(Figure 1).

Each plate is 200x50x1,8mm
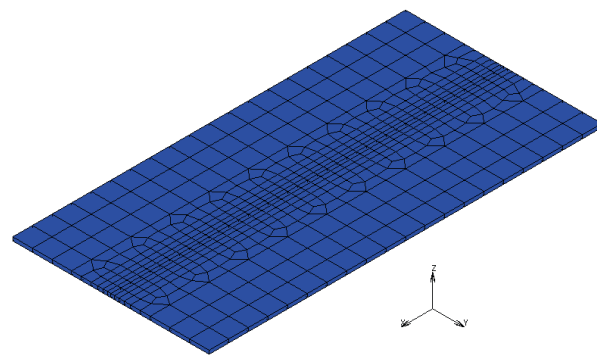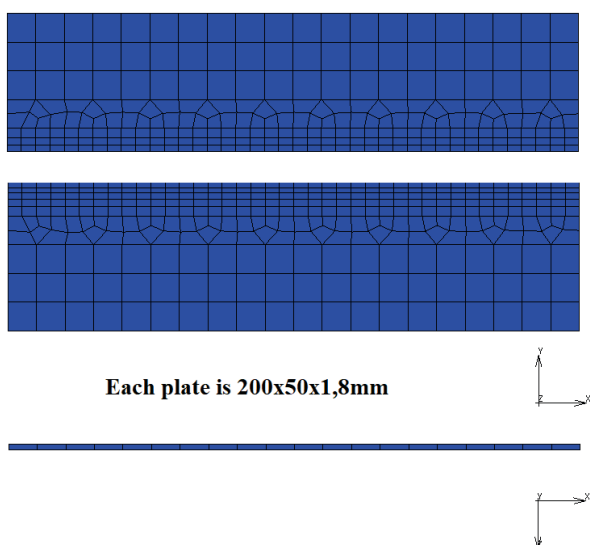
Fig. 1. *Meshed welded parts*

Note that additional support tools are often used in precision welding to clamp the shell or prevent out-of-plane movement. This also reduces buckling, especially when the sheets are thin. In this model, the panels are each 0.2 m long, 0.05 m wide and 0.0018 m thick.

Marc Mentat has different levels of material behaviors for modeling metals. In this example, the mechanical and thermal properties are temperature dependent, but the effect of phase change on mechanical properties is not included in the model. Steel is defined by the options isotropic, table and latent heat.

The plate is glued to the clamp to simplify the example problem. This is not a conventional method as it causes unnecessary thermal stress. Contact bodies are defined in the contact option. The interaction of these locations is defined with the con intera option. The two plates are in contact at the start of the analysis. When a heat source heats the bodies to a temperature that meets the temperature criteria of the selected heat-driven bonding option, they bond during the analysis. This data is provided via the con intera option. Additional physical structural properties are not defined, but there is convection from the plate to ambient, which is room temperature. This data is in the contact option. The option 'Bonding over a temperature threshold paired with a peak temperature' is utilized. The peak temperature criteria assures that the material reached 1300°C during the study, regardless of whether the bodies were in touch or not. The temperature threshold, on the other hand, guarantees that when the two bodies come into touch, they are still warm enough to bind. The temperature and the peak temperature are both mean values between the temperatures of the

touching body and the temperatures of the touched body. Stress-free initial projection is enabled to compensate for any mistakes in mesh creation.

The thermal contact coefficient is 1000 W/m2 and is utilized before bonding occurs. The coefficient of close thermal contact is 50 W/m2. In theory, neither is necessary in this model because it is symmetric, but in practice, this is not the case.

The two plates' starting temperature is reported as 20°C. It is not essential to assign a fixed temperature or displacement to any node of the model since contact with the clamps ensures solution stability. A laser heater is moved around a curve along the plate's edge. The heat source is positioned in the negative z global direction, as indicated below. The Mentat menu, which is used to determine these

quantities, may also be seen. The weld path option in Marc is used to specify this.

The weld flux option controls the intensity of the source, its speed, and the shape/penetration level of the heat source. The heating source has a power output of 4000, 4200 and 4500 W. The heating source has two types of fluxes: surface fluxes and cylindrical volumetric fluxes. This is accomplished by applying the same power but assigning a surface flux efficiency of 4% and a volumetric flux efficiency of 96%. The source's velocity is 0.05 m/s.

CONCLUSION

Figure 2 shows the stress fields in the center plane of the weld during the 24 second period from the start of the welding process for the tested laser powers.
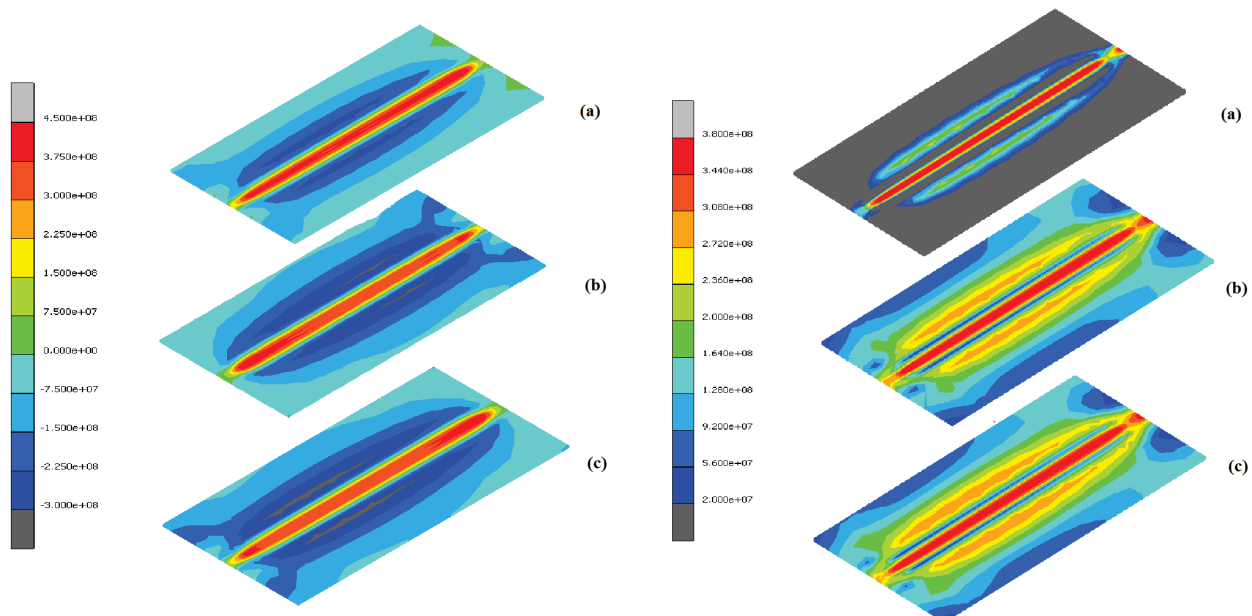
Fig. 2. Simulation results; C11stresses on the left, Von mises stresses on the right; (a)4000W, (b)4200W, (a)4500W

The variation of the stresses in the weld direction for each laser power is shown on the left side of Figure 2. The highest stress values have been reached for 4500W. Von mises stresses for each power value are shown on the right side. At low power values, a decrease was observed in the stress value in the regions far from the weld pool. At 4500W power, the dispersion around the weld pool is increasing.

Figure 3 shows the temperature change in the weld pool for 24 hours. At 4500W, the highest temperature of 1455 C was reached.

Figure 4 shows the residual stress change on an arc passing through the midpoint.

The main purpose of the article was to develop and apply a simulation model for the analysis of temperature fields during the formation of different Al7075 alloy weld joints to adjust the appropriate laser power using

numerical simulation in the MSC Marc Mentat program code.
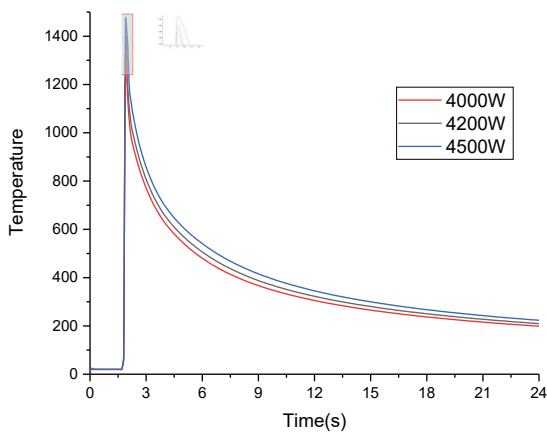
***Fig. 3.** Temperature variation during welding process*
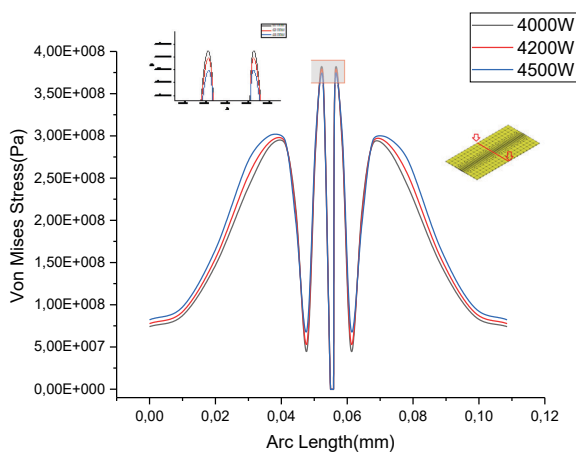
***Fig. 4.** Von Mises Stresses on mid-line of the weld*

It can also be assumed that the laser beam offset has a significant effect on the complete melting of materials and the production of high-quality weld joints. Therefore, the effect of laser beam offset on the temperature distribution in welded materials can be investigated in the next step. Finally, numerically optimized parameters will be used for the experimental fabrication of Al7075 alloy weld joints. Comparison of the obtained numerical results with the experimentally measured temperatures will be used to validate the developed simulation model.

REFERENCE

[1]Solana, P., Negro, G., 1997. A study of the effect of multiple reflections on the shape of the keyhole in the laser processing of materials. J. Phys. D: Appl. Phys. 30, 3216–3222.

[2]Okerblow, N., 1958. The Calculations of Deformations of Welded Metal Structures. Her Majesty's Stationery Office, London, UK. Masubuchi, K., 1980. Analysis of Welded Structures. Pergamon Press, Oxford, UK.

[3]Yang, L.J., Xiao, Z.M., 1995. Elastic–plastic modeling of theresidual stress caused by welding. J. Mater. Process. Technol. 48, 589–601.

[4]Tanigawa, Y., Akai, T., Kawamura, R., Oka, N., 1996. Transient heat conduction and thermal stress problems of a nonhomogeneous plate with temperature-dependent material properties. J. Therm. Stresses 19, 77–102.

[5]Chakravarti, L., Malik, M., Goldak, J., 1986. Prediction of distortion and residual stresses in panel welds. In: Computer Modeling of Fabrication Processes and Constitutive Behavior of Metals. Canadian Government Publishing Centre, Ottawa, Ontario, pp. 547–561.

[6]Fujii, S., Takahashi, N., Sakai, S., Nakabayashi, T., Muro, M., 2000. Development of 2D simulation model for laser welding. In: Proceedings of SPIE, vol. 3888.

[7]Frewin, M.R., Scott, D.A., 1999. Finite element model of pulsed laser welding. Weld. J. Weld. Res. Suppl. (January), 15s–22s. Reinhart, G., Lenz, B.,

[8]Rick, F., 1999. Finite element simulation for the planning of laser welding applications. In: Proceedings of the 18th International Congress on Applications of Lasers and Electro-Optics (ICALEO'99), San Diego, CA.

[9]Carmignani, C., Mares, R., Toselli, G., 1999. Transient finite element analysis of deep penetration laser welding process in a single-pass butt-welded thick steel plate. Comput. Methods Appl. Mech. Eng. 179, 197–214.

[10]Kang, D.-H., Son, K.-J., Yang, Y.-S., 2001. Analysis of laser weldment distortion in the EDFA LD pump packaging. Finite Elem. Anal. Des. 37, 749–760.

[11]Lankalapalli, K.N., Tu, J.F., Gartner, M., 1996. A model for estimating penetration depth of laser welding processes. Phys. D: Appl. Phys. 29, 1831–1841.

[12]Lampa, C., Kaplan, A.F.H., Powell, J., Magnusson, C., 1997. An analytical thermodynamic model of laser welding. Phys. D: Appl. Phys. 30, 1293–1299.

[13]Williams, K., 1999. Development of laser welding theory with correlation to experimental welding data. Laser Eng. 8, 197–214.

[14]Duley, W.W., 1999. Laser Welding. John Wiley & Sons, New York.

[15]Solana, P., Ocana, J.L., 1997. A mathematical model for penetration laser welding as a free-boundary problem. J. Phys. D: Appl. Phys. 30, 1300–1313.

394

[16]Kar, A., Mazumder, J., 1995. Mathematical-modeling of key-hole laser-welding. J. Appl. Phys. 78, 6353–6360.

[17]Dowden, J., Wu, S.C., Kapadia, P., Strange, C., 1991. Dynamics of the vapor flow in the keyhole in penetration welding with a laser at medium welding speeds. J. Phys. D 24, 519–532.

[18]Kar, A., Rockstroh, T., Mazumder, J., 1992. 2-dimensional model for laser-induced materials damage-effects of assist gas and multiple reflections inside the cavity. J. Appl. Phys. 71, 2560–2569.

[19]Metzbower, E.A., 1993. Keyhole formation. Met. Trans. B Process Met. 24, 875–880. Klein, T., Vicanek, M., Kroos, J., Decker, I., Simon, G., 1994. Oscillations of the keyhole in penetration laser-beam welding. J. Phys. D 27, 2023–2030.

[20]Matsunawa, A., Semak, V., 1997. The simulation of front keyhole wall dynamics during laser welding. J. Phys. D 30, 798–809.

[21]Kapadia, P., Solana, P., Dowden, J., 1998. Stochastic model of the deep penetration laser welding of metals. J. Laser Appl. 10, 170–173.

[22]Fabbro, R., Chouf, K., 2000. Keyhole modeling during laser welding. J. Appl. Phys. 87, 4075–4083.

[23]Rosenthal, D., 1946. The theory of moving sources of heat and its application to metal treatments. Trans. Am. Soc. Mech. Eng. 68, 849–866.

[24]Swift-Hook, D.T., Gick, A.E.F., 1973. Penetration welding with lasers. Weld. Res. Suppl., 492s–498s.